SAR Journal of Medical Biochemistry

Abbreviated Key Title: *SAR J Med Biochem*
Home page: https://sarpublication.com/journal/sarjmb/home
DOI: https://doi.org/10.36346/sarjmb.2024.v05i06.001

OPEN ACCESS

ISSN 2707-7721 (P)
ISSN 2709-6882 (O)

Original Reserach Article

Stabilized Gold Nanoparticles on α-Hydroxy Amide-Functionalized Graphene Oxide as a Robust Catalyst for Environmentally Benign Oxidation of Primary and Secondary Alcohols

Dalia Sadiq Mahdi AL-Khateeb[1*], Heshmatollah Sepahvand[1]
[1]Applied Biotechnology Department, College of Biotechnology, Al -Qasim Green University Babylon 51013, Iraq
[2]Shahid Behshi University, Tehran, Iran

***Corresponding Author:** Dalia Sadiq Mahdi AL-Khateeb
Applied Biotechnology Department, College of Biotechnology, Al -Qasim Green University Babylon 51013, Iraq

Article History: | Received: 08.11.2024 | Accepted: 13.12.2024 | Published: 28.12.2024 |

Abstract: Multi-component reactions (MCRs), one of the most powerful approaches to synthesizing complexstructures from the fastest path, have grabbed much attention and have recently been used to functionalize the surface of nanomaterials. Here, we focus on an isocyanide-based multi- component reaction for one-pot functionalization of the graphene oxide surface. This led to α- hydroxy amide decorated graphene oxide with the ability to immobilize Gold nanoparticles and serve as a neoteric catalytic system. This nanocatalyst was characterized by means of SEM, TEM,ICP-OES, FTIR, XRD, Raman, and BET techniques. This employed multifunctional nanostructure as an efficient and recyclable heterogeneous aerobic catalyst for the oxidation of primary and secondary aliphatic and aromatic alcohols to their aldehydes and ketones in water at mild temperature in good to excellent yields. Further, this method showed that recycling of heterogeneous catalysts has a high possibility of being re-used with their performances as it was new with no sign of gold leaching.

Keywords: Multifunctionalized Graphene Oxide, Isocyanide, Stablized Gold NPs, Green Oxidation, Aerobic, Alcohols.

INTRODUCTION

Recently, graphene-based nanosheets have been widely used as support materials for biomedical applications as well as catalytic demands such as drug delivery, biosensing, bioimaging, enzyme immobilization, and organic transformations [1]. Graphene-based nanomaterials have interesting mechanical, chemical, thermal, electrical, and optical properties [2]. However, the use of these materials has been limited due to safety concerns about their instability and toxicity in physiological conditions, and low dispersity in aqueous media. The functionalization and modification of the surfaces of the graphene-based materials are effective strategies to improve their properties consisting of aqueous dispersity, physiological stability, and toxicity [3]. In addition, these strategies produce the additional diverse functional groups on the sheet surfaces as active sites for the interaction with metal and/or organic substrates; accordingly, the capacity and adsorption capability of the graphene-based nanomaterials for catalytic and biological applications [4]. Graphite is a 3D layered structure of the graphene sheets, whereby each layer can dissociate from each other by the van der Waals forces. The graphene based materials were synthesized from graphite through oxidation in an acid environment known as exfoliation of graphite which imparted the graphene oxide sheets with hydroxyl, epoxide, carbonyl and carboxyl functionalities on the surface of the graphene sheets [4, 5]. Furthermore, the oxidation process produces defects in the sheets consisting of defects in □ bonds and □ bonds lattices. The □ defects are the vacancy in the graphene oxide sheet as a result of over-oxidation and CO2 releasing, and the defects are the sp^3 carbon atoms (the functional groups-attached carbon atoms) that lie out-of-the plane. In general, the modification of the graphene oxide sheets was achieved

by altering the synthesis method as well as the functional groups found in the sheet [6]. According to the modification processes, the amounts and types of the functional groups of the graphene oxide sheets were varied; for instance, reduced and aminated graphene oxide [7]. Because of the presence of the various functional groups on the graphene oxide sheets, they readily undergo organically functionalization. There are several ways of organizing the functionalization of the surface of Graphene Oxide sheets with synthetic and natural polymers, organic compounds and biological molecules [3-8].

As oncoming field nanotechnology is about to bring basic changes in generating and will make a profound impact on every part of catalytic applications specifically drug delivery, cancer therapy, adsorption, and organic transformations [9]. As the development of the nanotechnology over last decade, different types and shapes of nanosize materials have been synthesized such as metal, metal oxide, and polymeric nanoparticles (NPs) [10]. By controlling the size, shape, and morphology of the nanoparticles, the surface characteristics, as well as specific surface area of the nanoparticles, can be specialized. According to this development in nanotechnology, various types of NPs and modified/functionalized NPs have been utilized as a catalyst [11]. The gold NPs in different shapes and sizes are important tools for catalysis utilities due to their unique surface activity, stable and nontoxic nature. Among the techniques of preparation of the gold NPs is the use of trisodium citrate acting both as reducer and capping agent from the preparation of HAuCl4 but the method has drawbacks in that it is unable to stable NPs for the long time under high concentration status of more than 200ppm. The catalytic activity of gold NPs completely deteriorate when their size is reduced to micro meters so in order to avoid the agglomeration of gold NPs these were synthesized on supports and later stabilized with a layer of polymers or surfactants [12]. Continuing our work on design and synthesis of the organically functionalized nanocomposites, we planned and synthesized a new multifunctional GO: AuNp hybrid system started from amine-modified GO and examined its proficiency to catalyze the oxidation of the primary and secondary alcohols using a green protocol in aqueous medium.

EXPERIMENTAL SECTION MATERIAL AND METHODS

The far-infrared spectra were obtained on a Ray Leigh Wqf-510 FT-IR spectrophotometer. Both SEM and EDX tests were done using Philips XL-300 equipment. Stereo-TEM was performed using CM10 Philips electron microscope in at mode. X-ray diffraction measurements were conducted on Philips-X'pert Pro (PW 3040) X ray diffractometer with wave length of monochromatic Cu-Kα radiation, k = 1.54056 Å, voltage = 40 kV and current = 30 mA. Surface characteristics of as-prepared samples were assessed from the N2 adsorption at a temperature of −196°C in Micromeritics TriStar ASAP 3000 instrumental setup using BET technique. Determination of the concentration of gold was made analytically using (ICP-OES) Varian Vista PRO Radial model. All the chemical reagents and solvents used in this work were purchased from Fluka, Merck and Aldrich and as such no further purification was done.

Preparation of Amino Graphene Oxide (AGO)

The graphene oxide (GO) sheets were prepared by the modified Hummer's method [4d]. Briefly, GO (0.1 g) was dispersed into ethylene glycol (50 mL) by sonication for 30 min to prepare a 2 g/L GO solution. Then, 1.0 mL of ammonia solution (25%) was added to the GO solution, and the reaction mixture was continued overnight at 80 ºC. The solid products (AGO) were collected by centrifuging, washing with deionized water/ethanol (1:1, 5 mL), and drying at 50 °C under vacuum for 6 h.

Preparation of α-Hydroxy Amide Functionalized Graphene Oxide (AAGO)

To the solution of amino graphene oxide (0.10 g) in acetonitrile (20 mL), epichlorohydrin (0.03 g, 0.30 mmol) and triethylamine (0.01 mL) were added and stirred for 10 h at 50 ºC. After this time, the solvent was evaporated under reduce pressure and the residue solid was used for next step. The obtained functionalized graphene oxide (EAGO) was poured into a solution of tetrahydrofuran/ deionized water (9:1, 20 mL) containing of 0.100 g of *p*-toluenesulfonylmethyl isocyanide (TosMIC) and 0.001 g InCl3, and then, the reaction mixture was refluxed for 6 h at 100 ºC under magnetically stirring. The reaction product (AAGO) was collected by centrifuging and purified by washing three times with water/ethanol (1:1, 5 mL) and dried at 50 ºC under vacuum for 6 h.

Immobilization of gold NPs on the surface of AAGO

The solution of the HAuCl4 (3.0 mmol), polyethylene glycol (0.30 g, MW=20,000), and trisodium citrate (24.0 mmol) in water (300 mL) was heated under microwave irradiation to 60 ºC for 10 min as long as it is magnetically stirred. Then, 3.0 mL of the obtained solution was diluted with 30 mL of deionized water, charged by 0.30 g of AAGO and stirred for 10 h at ambient temperature. The final product (Au/AAGO, 0.33 g) was collected, washed and dried as same as previous steps. The loading of gold was obtained 0.07 mmol g^{-1} by ICP-OES.

Au/AAGO Catalyzed Oxidation of Alcohols Follows a General Procedure Mentioned Below

An alcohol (1.0 mmol), KOH (1.0 mmol) and Au/AAGO (0.02 g) was added into a round bottom flask containing 3 mL of water and reaction mixture was stirred at a certain temperature under O2(1 atm) for 4-12 h. The scale of the reaction was measured using GC with an internal standard. At the end of the given reaction, the

catalyst was removed by using centrifugal force, and the efficiency of the product formation was investigated by GC.

RESULTS AND DISCUSSION

The functionalization of nanostructures is utilized to modify their properties. Herein, we functionalized the graphene oxide surface with the aim of increasing the dispersity of this system in the aqueous medium as well as creating a stronger interaction of the support with the gold nanoparticles and the raw materials in the organic transformations. A new multifunctional graphene oxide@gold nanocomposite was synthesized through the multi-step process. Initially, graphene oxide (GO) was synthesized using graphite by an exfoliation process, then the GO surface was modified with amino groups (AGO). The amino-modified GO was functionalized by epichlorohydrin (EAGO) and following by reaction with *p*-toluenesulfonylmethyl isocyanide (TosMIC) to provide □-hydroxy amide functional groups on the GO sheets (AAGO) [14]. The AAGO has different functional groups such as amino, hydroxyl, amide, epoxy, and □-hydroxy amide groups; accordingly, it is suitable to stabilize metal nanoparticles. The gold NPs were immobilized on the AAGO sheets (Au/AAGO). Modified graphene materials, including graphene oxide, have defects in their sp^2 lattice, which the areas of defects have a greater potential to stabilize the supported materials (gold nanoparticles in this article), so functionalization of the graphene oxide surface with a bidentate organic ligand, it prevents the accumulation and aggregation of gold nanoparticles on the surface and helps to distribute the particles uniformly.

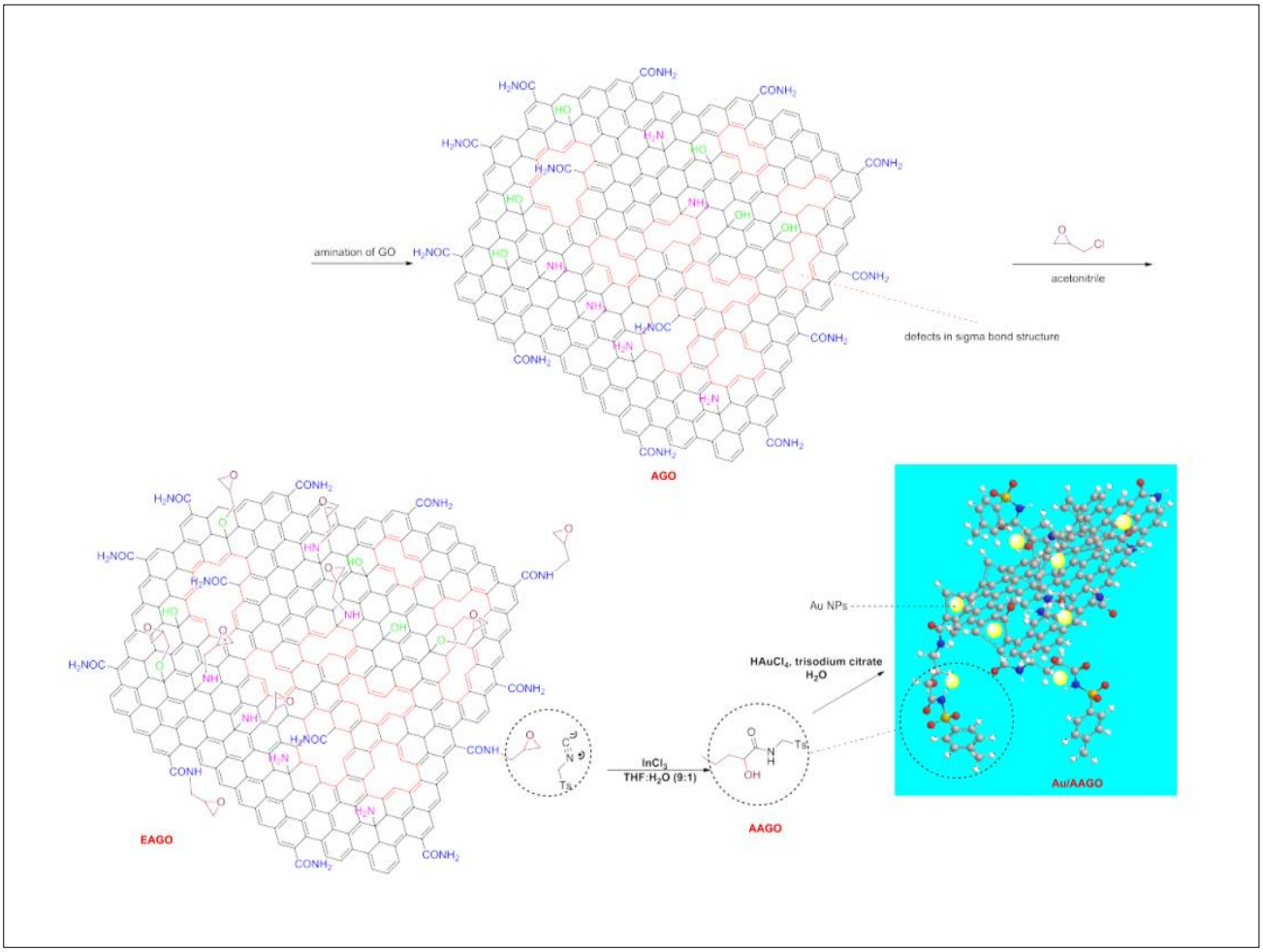

Scheme 1: Synthesis of the α-hydroxy amide-functionalized graphene oxide-gold nanocomposite

The Au/AAGO was characterized by SEM images that were shown in Fig. 1. The Au/AAGO SEM images shown the wrinkled sheets with rough morphology, which the sheet surfaces details were observed in the magnified SEM image. The TEM images of Au/AAGO confirmed the existence of a composites structure that the Au NPs were uniformly dispersed on the AAGO sheets and also the monolayer structure of the AAGO sheets. The average size of the Au NPs is around 15-17 nm. As seen in the HR-TEM images, the gold NPs have nanocage or nanocluster structures. The SEM mapping and EDX analysis showed the existence of the C, N, O, and Au elements that confirmed the desirable composition of the Au/AAGO.

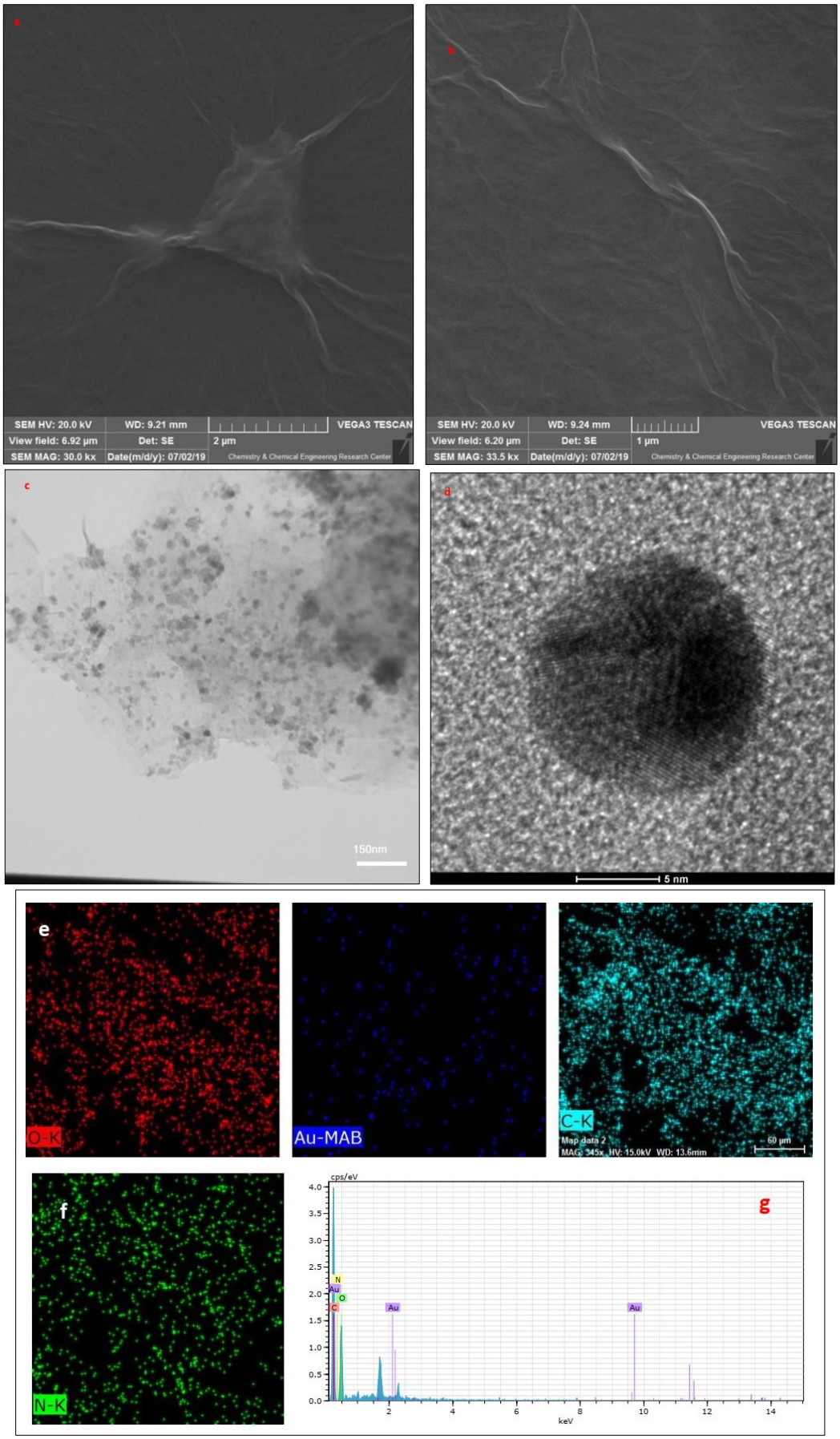

Figure 1: The SEM images (a and b), TEM images (c and d), SEM mapping images (e and f), and EDX analysis (g) of Au/AAGO

The FTIR spectra of GO and functionalized GO were shown in the Fig. 2. The characteristic functional groups in the structure of GO were identified through the characteristic stretching vibrations of C=C and C=O bonds in the range of 1580-1720 cm- and above 3000 cm^{-1}, respectively as noted in the literature.[15] Characterizations of functional groups spectra were; 3400-3500 cm-1 for v OH or NH; 3000-3100 cm-1.vmCHaliph; 1700 cm-1vC=O Amino; 1500- 1600 cm^{-1} for -NH2 bend; 1285-1350 cm -1 for -OH bend; 1010-1250 cm-1 The stretching vibrations of N-H at 3300-3500 cm^{-1}, S=O at 1050 cm-1 and C-H at 2800-3000 cm-1 testified to the successful grafting of functional groups on to GO.

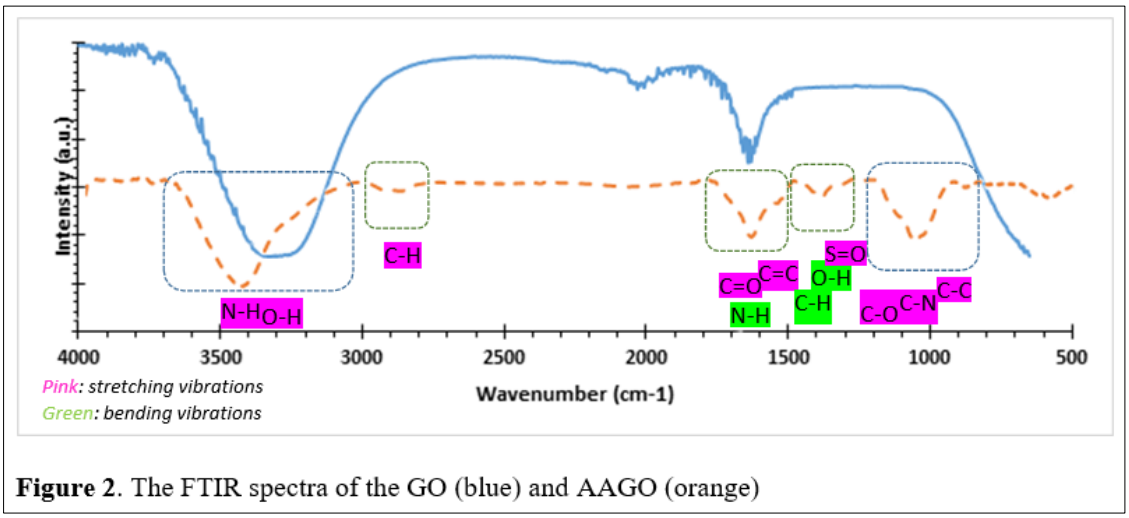

Figure 2. The FTIR spectra of the GO (blue) and AAGO (orange)

The XRD pattern of the GO and AAGO were provided that shown in Fig. 3. The characteristic diffraction peaks of the GO are observed in both of them that they are verified the stability of the GO structure during the modification and functionalization processes [17]. As seen in the AAGO pattern, the new diffraction peaks have emerged that are in agreement with gold NPs diffraction peaks [12b].

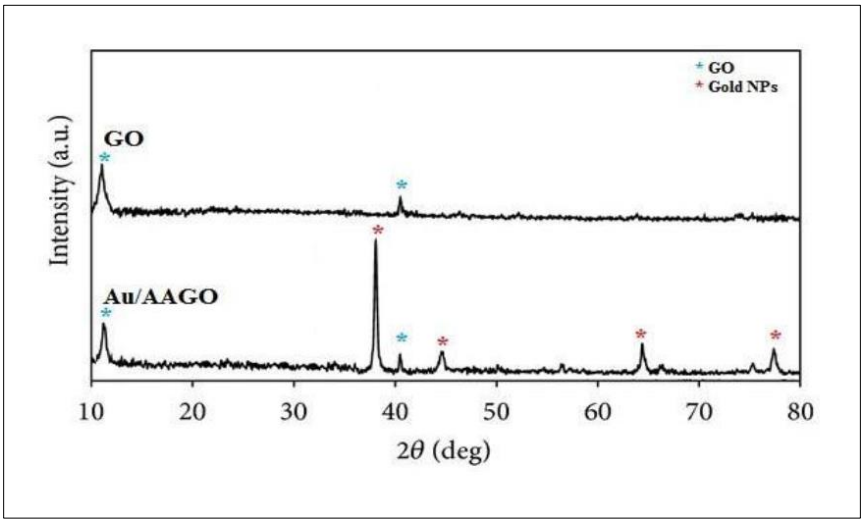

Figure 3: The XRD patterns of the GO and Au/AAGO

Raman spectroscopy is used for distinguishing ordered, and disordered crystal structure of carbon materials as a typical technique. The Raman spectra of GO, AAGO and Au/AAGO composites have been shown in Fig. 4. Typically G band is usually assigned to sp^2 hybridized carbon atoms (E2g phonon), while the D band is correlated to disorder and local defects (breathing-point phonon with A1g symmetry). As seen in all spectra, two main peaks are observed located at around 1350 cm^{-1} and 1600 cm^{-1} corresponding to D and G bonds, respectively. The ratio of D and G bonds intensities (ID / IG) evaluates the crystalline structures of carbon materials. The ID / IG values for GO, AAGO, and Au/AAGO are 0.92, 1.08, 1.23, respectively, which are corresponding to an increase of defects (or attached sites) in the GO sheets during functionalization and gold NPs immobilization [18].

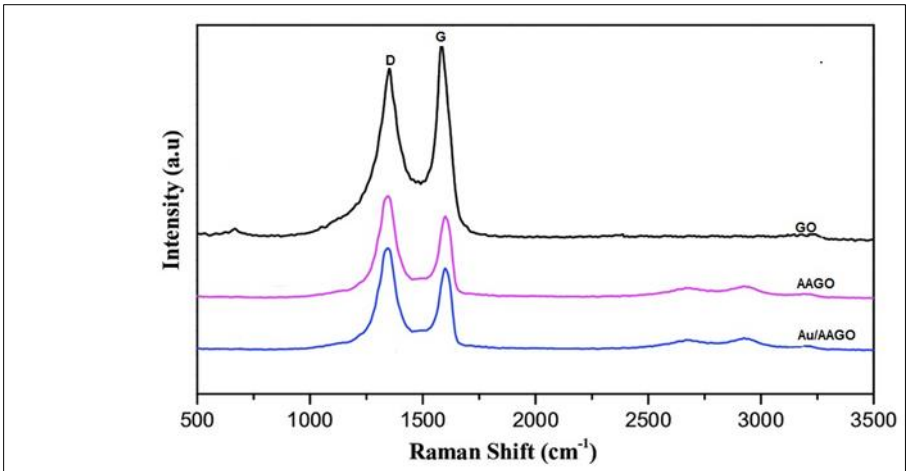

Figure 4. The Raman spectra of the GO, AAGO, and Au/AAGO

The specific surface area of the GO, AAGO, and Au/AAGO was measured by the BET method with N2 adsorption–desorption at −196°C, and the curves were shown in Fig. 5. The BET surface area of GO is 137.4 m^2g^{-1} which decreased to 44.2 m^2g^{-1} and 35.3 m^2g^{-1} for AAGO and Au/AAGO, respectively. The results show that the surface area of the GO is decreased during functionalization and gold NPs immobilization due to the filling of the GO attached sites with organic functional groups and gold NPs.

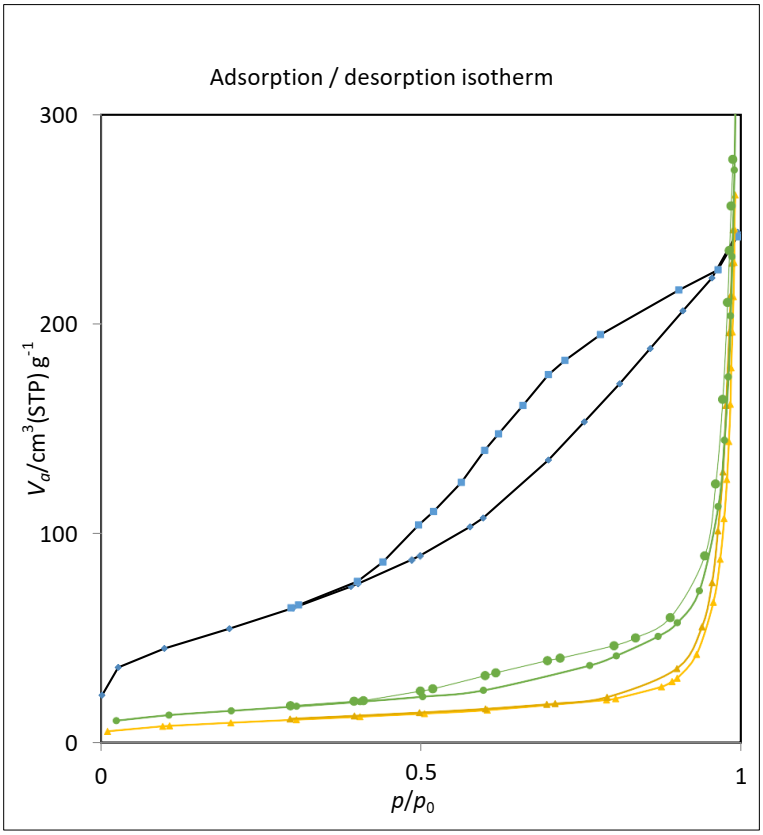

Figure 5: The BET analysis of the GO, AAGO, and Au/AAGO

The catalitical activity of the Au/AAGO was determined by the oxidation reaction of the primary and secondary alcohols. To identify a green method, the investigations were begun with the oxidation reaction of the benzyl alcohol under aerobic environment. The oxidation reaction was carried out with benzyl alcohol (1.0 mmol) using Au/AAGO (0.02 g) catalyst and carried in 3 mL water as solvent under air reflux conditions. The first reaction slightly produced the benzaldehyde as the desired product at room temperature within 12h less than 10%, in line with this the reaction temperature was gradually increased to 100 °C. When the reaction

temperature was raised, the reaction yield was enhanced in an optimal manner up to 29% at 100 oC. Subsequently, the higher temperatures were also analyzed here, but the yields were not introduced here, as there was no substantial difference in the yields. Subsequently, the dependence of the inorganic bases (from the environmental perspective) was studied for the oxidation of benzyl alcohols. Different bases including KOH, K2CO3, KHCO3, and Na2CO3 were employed on the oxidation reaction of the benzyl alcohol, with an optimal yield of 90% given at 70 oC using KOH after a 6h reaction period. In addition, the O2 gas was used as an oxidant instead of air, which the reaction yield was increased to 92% under O2 atmosphere under same conditions. Similarly, hydrogen peroxide and *tert*-butyl hydrogen peroxide (TBHP) were examined that shown the results closed to O2. Finally, the air, KOH, water, and 70 °C were chosen as optimum oxidant, base, solvent, and reaction temperature, respectively. In all optimization reactions, the existence of the benzoic acid in the products was investigated after neutralization.

Table 1. Optimization of the benzyl alcohol oxidation reaction conditions[a]

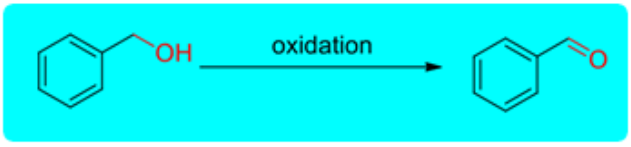

Entry	Catalyst (g)	Oxidant	Solvent	Base	Temperature (°C)	Time (h)	Yield (%)[b]
1	Au/AAGO (0.02)	Air	H_2O	-	25	12	<10
2	Au/AAGO (0.02)	Air	H_2O	-	50	6	24
3	Au/AAGO (0.02)	Air	H_2O	-	100	6	29
4	Au/AAGO (0.02)	Air	H_2O	KOH	50	6	38
5	Au/AAGO (0.02)	Air	H_2O	KOH	70	6	90
6	Au/AAGO (0.02)	Air	H_2O	KOH	100	6	90
7	Au/AAGO (0.02)	Air	H_2O	K_2CO_3	70	6	41
8	Au/AAGO (0.02)	Air	H_2O	$KHCO_3$	70	6	40
9	Au/AAGO (0.02)	Air	H_2O	Na_2CO_3	70	6	35
10	Au/AAGO (0.01)	Air	H2O	KOH	70	6	30
11	Au/AAGO (0.03)	Air	H2O	KOH	70	6	82
12	Au/AAGO (0.02)	O2	H2O	KOH	100	4	83c
13	Au/AAGO (0.02)	O2	H2O	KOH	70	4	92
14	Au/AAGO (0.02)	H2O2 (1 equiv.)	H2O	KOH	70	10	76
15	Au/AAGO (0.02)	TBHP (1 equiv.)	H2O	KOH	70	10	93
16	AAGO (0.02)	Air	H2O	KOH	70	12	-
17	Au NPs	Air	H2O	KOH	70	12	35

[a]Reaction conditions: Benzyl alcohol (1.0 mmol), base (1.0 mmol) and solvent (3 mL); [b]GC determinedyields; [c]Benzoic acid was prepared ~10%.

To confirm the Au/AAGO catalysis activity and also to clarify the main catalyst species, the oxidation reaction was repeated in absence of gold NPs (AAGO) that the reaction did not carry out. As complementary study, the reaction with gold nanoparticles was performed in parallel under the same conditions as the optimal state, which had a very low efficiency, which confirms the synergistic effects of graphene support on the activity of gold nanoparticles. This synergistic effect can result from the uniform distribution of gold particles

on the surface of graphene oxide and the intermolecular interactions of the surface functions of the graphene structure with the raw materials molecules.

With the optimum conditions in hand, different derivatives of the benzyl alcohols were oxidized in the presence of Au/AAGO nanocomposites. As seen in Scheme 2, the oxidation reactions of the electron-donating substituted derivatives obtained more yields than others, exceptionally, the 4- methoxy and 4-nitro derivatives did not go through this flow. According to the main catalysis role of gold NPs and the Au content of Au/AAGO, determined by ICP-OES data, the TOF (h) number of each reaction was determined.

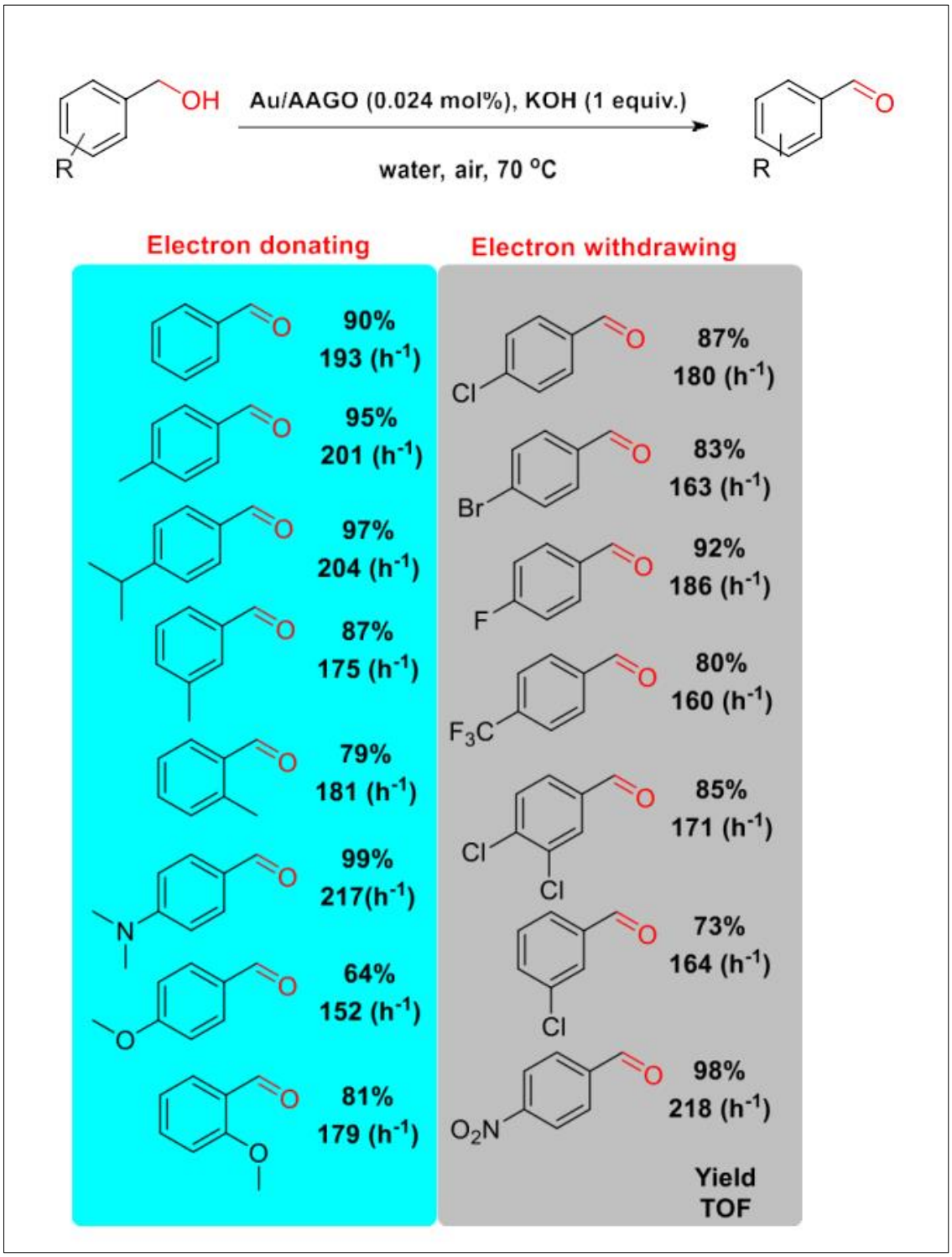

Scheme 2: Oxidation of the benzyl alcohols

Because of the high catalytic activity of the Au/AAGO in the aerobic oxidation of benzyl alcohols, this oxidation process was now applied to aliphatic primary alcohols. When other aliphatic primary alcohols were tested under the above optimum conditions, these reactions yielded moderate to good results in 8-10 h. However, when the reaction temperature was increased to 100 oC, only a slightly better yield of the oxidation reactions was obtained. It also, has illustrated in Scheme 3 the structural features of the products that this scheme tried to highlight.

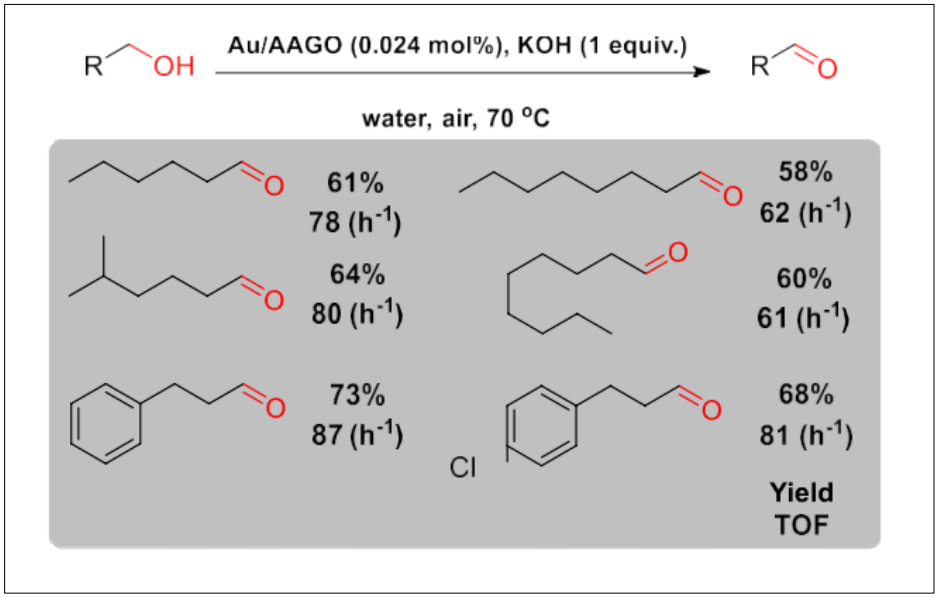

Scheme 3: Oxidation of the aliphatic primary alcohols

As the second part of the study on the Au/AAGO catalytic activity, its activity was investigated in secondary alcohols oxidations, started with 1-phenylethanol as a model compound. Fortunately, this process efficiently oxidized the 1-phenylethanol into acetophenone with 99% yield in 7 h at 100 °C. Next, the various derivatives of the secondary alcohols were successfully used (Scheme 4).

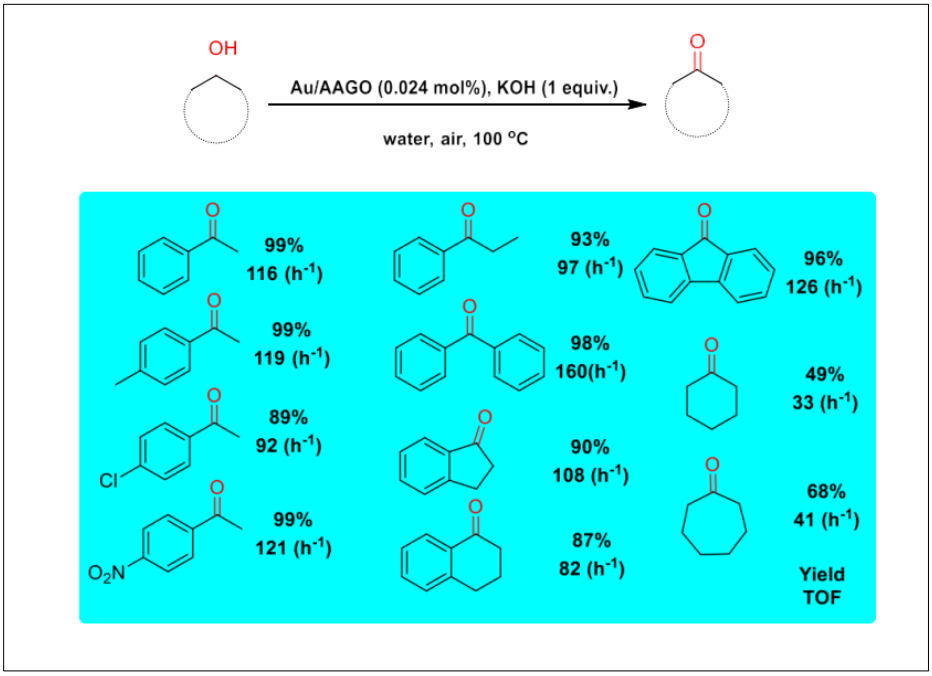

Scheme 4: Oxidation of the secondary alcohols

The stability of the gold NPs on the Au/AAGO catalyst surface was estimated by a hot filtration test during the oxidation of the benzyl alcohol under the optimized conditions. Additionally, the catalyst recyclability and reusability were investigated in benzyl alcohol oxidation as a model reaction for five repetitive

cycles including the separation of the catalyst by centrifuging, washing three times by water and ethanol, and dried at 100 ºC after each oxidation reaction cycle. Fortunately, this catalyst displayed excellent efficiency as same as the first time use (Fig. 6).

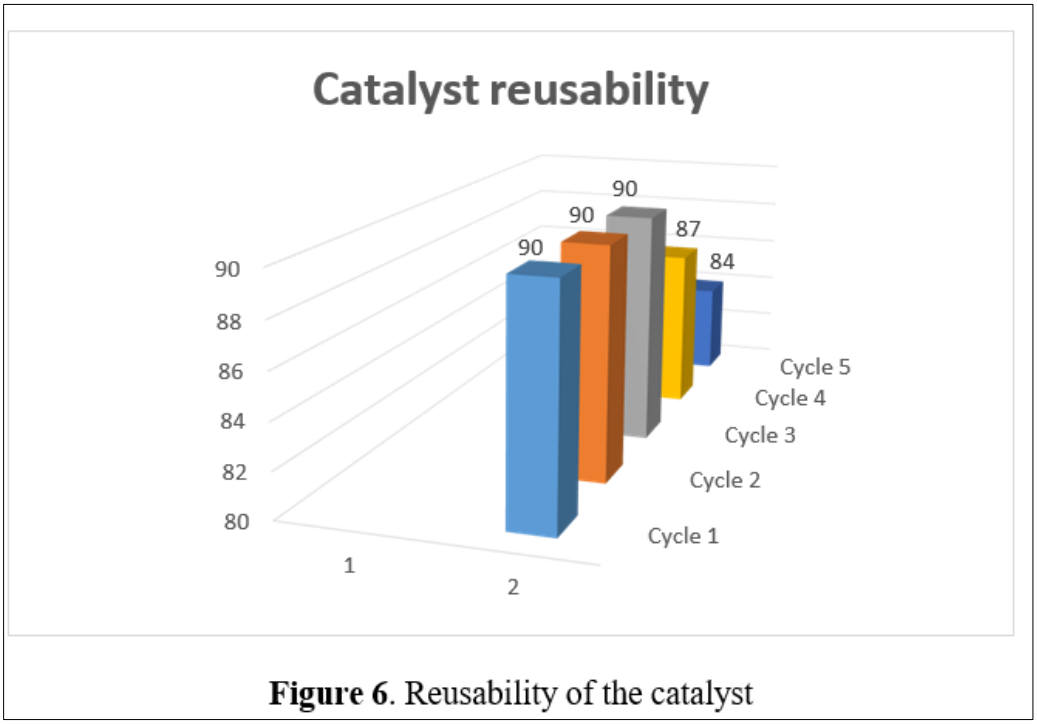

Figure 6. Reusability of the catalyst

The possible mechanism for the oxidation of the benzyl alcohol has been depicted in Scheme 5. As seen in the mechanism, the supported gold NPs surfaces interact with singlet oxygen molecules that provide the peroxy radical intermediates on these surfaces, and then the radicals attack the acidic hydrogen of the alcohol hydroxyl groups to form the alkoxy radicals, which subsequently absorb on the gold NPs surfaces (oxidative addition of O2 and alcohol radical on the gold NPs as a three-component intermediate). Finally, by the participation of the base in the reaction, an alcohol carbanion is formed from the intermediate following by a reduction elimination reaction, and benzaldehyde and hydrogen peroxide are produced.

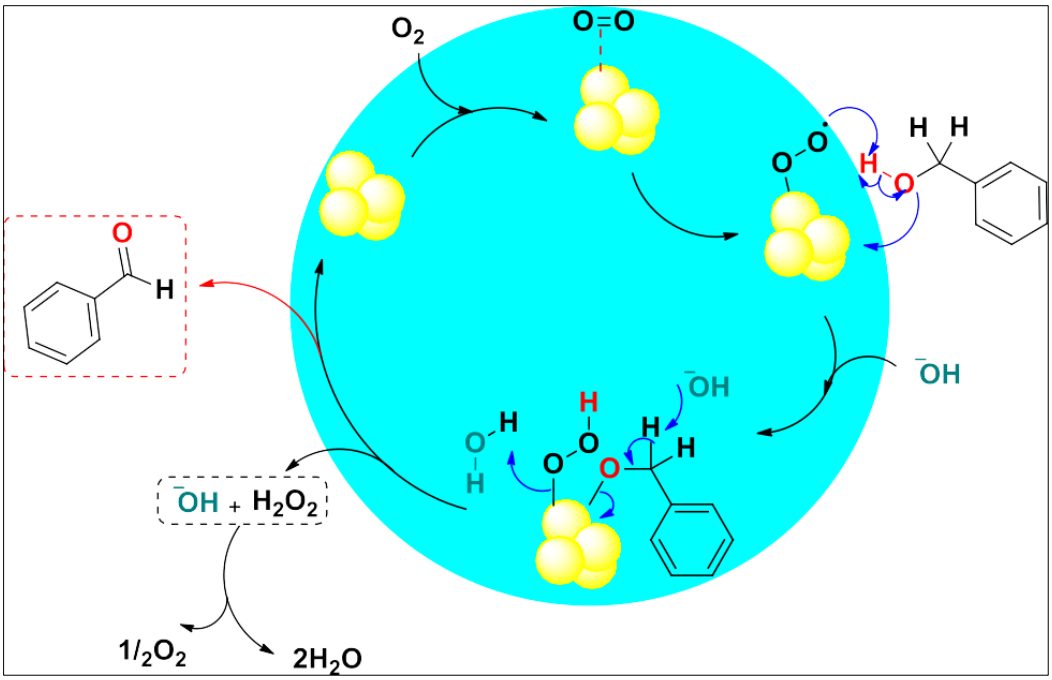

Scheme 5: The proposed mechanism of the benzyl alcohol oxidation

CONCLUSION

In summary, this research reported on design, preparation, and characterization of a new multifunctional graphene oxide composite containing gold NPs. This composite structure was used as an efficient, reusable, and stable heterogeneous catalyst for the aerobic oxidation of various types and derivatives of aliphatic and aromatic alcohols through the green procedures in water under mild conditions.

ACKNOWLEDGMENTS

We acknowledge the financial support of this work, provided by the Science and Research Branch of the Islamic Azad University in Tehran.

REFERENCES

1. Zhu, Y., Murali, S., Cai, W., Li, X., Suk, J. W., Potts, J. R., & Ruoff, R. S. (2010). *Advanced materials*, *22*, 3906-3924, Chung, C., Kim, Y. K., Shin, D., Ryoo, S. R., Hong, B. H., & Min, D. H. (2013). *Accounts of chemical research*, *46*, 2211-2224, Dimiev, A. M., Eigler, S. (2016). *Graphene oxide: fundamentals and applications*, John Wiley & Sons.
2. Suk, J. W., Piner, R. D., An, J., & Ruoff, R. S. (2010). *ACS nano*, *4*, 6557-6564, Gómez-Navarro, C., Weitz, R. T., Bittner, A. M., Scolari, M., Mews, A., Burghard, M., & Kern, K. (2007). *Nano letters*, *7*, 3499-3503.
3. Yu, W., Sisi, L., Haiyan, Y., & Jie, L. (2020). *RSC Advances*, *10*, 15328-15345, Wang, Y., Li, Z., Wang, J., Li, J., , Lin, Y. (2011). *Trends in biotechnology*, *29*, 205-212, Chen, D., Feng, H., & Li, J. (2012). *Chemical reviews*, *112*, 6027-6053.
4. Zhang, Y., Wu, C., Guo, S., & Zhang, J. (2013). Interactions of graphene and graphene oxide with proteins and peptides. *Nanotechnology Reviews*, *2*(1), 27-45.
5. Tournus, F., Latil, S., Heggie, M. I., & Charlier, J. C. (2005). π-stacking interaction between carbon nanotubes and organic molecules. *Physical Review B—Condensed Matter and Materials Physics*, *72*(7), 075431. Soleimani, E., Naderi Namivandi, M., & Sepahvand, H. (2017). ZnCl2 supported on Fe3O4@ SiO2 core–shell nanocatalyst for the synthesis of quinolines via Friedländer synthesis under solvent-free condition. *Applied Organometallic Chemistry*, *31*(2), e3566. Sepahvand, H., Ghasemi, E., Sharbati, M., Mohammadi, M. S., Pirlar, M. A., & Shahverdizadeh, G. H. (2019). The magnetic graphene oxide/NHC catalyzed aerobic direct amidation and cross-dehydrogenative coupling of aldehydes. *New Journal of Chemistry*, *43*(42), 16555-16565.
6. JM, M. D. K. D. B. (2010). Sinitskii A. *Sun Z. Slesarev A. Alemany LB Lu W. Tour JM Improved synthesis of graphene oxide. ACS Nano*, *4*(8), 4806-4814. Alam, S. N., Sharma, N., & Kumar, L. (2017). Synthesis of graphene oxide (GO) by modified hummers method and its thermal reduction to obtain reduced graphene oxide (rGO). *Graphene*, *6*(1), 1-18.
7. Sun, L. (2019). Structure and synthesis of graphene oxide. *Chinese Journal of Chemical Engineering*, *27*(10), 2251-2260. Dolbin, A. V., Khlistyuck, M. V., Esel'son, V. B., Gavrilko, V. G., Vinnikov, N. A., Basnukaeva, R. M., ... & Benito, A. M. (2016). The effect of the thermal reduction temperature on the structure and sorption capacity of reduced graphene oxide materials. *Applied Surface Science*, *361*, 213-220. Pan, X., Yang, M. Q., & Xu, Y. J. (2014). Morphology control, defect engineering and photoactivity tuning of ZnO crystals by graphene oxide–a unique 2D macromolecular surfactant. *Physical Chemistry Chemical Physics*, *16*(12), 5589-5599.
8. Gong, X., Liu, Y., Wang, Y., Xie, Z., Dong, Q., Dong, M., ... & Guo, Z. (2019). Amino graphene oxide/dopamine modified aramid fibers: Preparation, epoxy nanocomposites and property analysis. *Polymer*, *168*, 131-137. Ramezanzadeh, B., Niroumandrad, S., Ahmadi, A., Mahdavian, M., & Moghadam, M. M. (2016). Enhancement of barrier and corrosion protection performance of an epoxy coating through wet transfer of amino functionalized graphene oxide. *Corrosion Science*, *103*, 283-304.
9. Sherlala, A. I. A., Raman, A. A. A., Bello, M. M., & Asghar, A. (2018). A review of the applications of organo-functionalized magnetic graphene oxide nanocomposites for heavy metal adsorption. *Chemosphere*, *193*, 1004-1017.
10. Barreto, J. A., O'Malley, W., Kubeil, M., Graham, B., Stephan, H., & Spiccia, L. (2011). Nanomaterials: applications in cancer imaging and therapy. *Advanced materials*, *23*(12), H18-H40. Yang, G., Zhu, C., Du, D., Zhu, J., & Lin, Y. (2015). Graphene-like two-dimensional layered nanomaterials: applications in biosensors and nanomedicine. *Nanoscale*, *7*(34), 14217-14231.
11. Cao, G. (2004). *Nanostructures & nanomaterials: synthesis, properties & applications*. Imperial college press. Vollath, D. (2008). *Environmental Engineering and Management Journal*, *7*, 865-870, Kolahalam, L. A., Viswanath, I. K., Diwakar, B. S., Govindh, B., Reddy, V., & Murthy, Y. L. N. (2019). Review on nanomaterials: Synthesis and applications. *Materials Today: Proceedings*, *18*, 2182-2190.
12. Somorjai, G. A., & Chaudret, B. (2012). *Nanomaterials in Catalysis*. John Wiley & Sons. Hu, M., Yao, Z., & Wang, X. (2017). Graphene-based nanomaterials for catalysis. *Industrial & Engineering Chemistry Research*, *56*(13), 3477-3502.
13. Brust, M., Fink, J., Bethell, D., Schiffrin, D. J., & Kiely, C. (1995). Synthesis and reactions of functionalised gold nanoparticles. *Journal of the Chemical Society, Chemical Communications*, (16), 1655-1656. Aromal, S. A., Vidhu, V. K., & Philip,

D. (2012). Green synthesis of well-dispersed gold nanoparticles using Macrotyloma uniflorum. *Spectrochimica Acta Part A: Molecular and Biomolecular Spectroscopy*, *85*(1), 99-104. Nghiem, T. H. L., La, T. H., Vu, X. H., Chu, V. H., Nguyen, T. H., Le, Q. H., ... & Tran, H. N. (2010). Synthesis, capping and binding of colloidal gold nanoparticles to proteins. *Advances in Natural Sciences: nanoscience and nanotechnology*, *1*(2), 025009. Sau, T. K., & Murphy, C. J. (2004). Room temperature, high-yield synthesis of multiple shapes of gold nanoparticles in aqueous solution. *Journal of the American Chemical Society*, *126*(28), 8648-8649.

14. Mirzaei, F., Mohammadi Nilash, M., Sepahvand, H., Fakhari, A. R., & Shaabani, A. (2020). Magnetic solid-phase extraction based on fluconazole-functionalized Fe3O4@ SiO2 nanoparticles for the spectrophotometric determination of cationic dyes in environmental water samples. *Journal of the Iranian Chemical Society*, *17*(7), 1591-1600. Shaabani, A., Sepahvand, H., Hooshmand, S. E., & Borjian Boroujeni, M. (2016). Design, preparation and characterization of Cu/GA/Fe3O4@ SiO2 nanoparticles as a catalyst for the synthesis of benzodiazepines and imidazoles. *Applied Organometallic Chemistry*, *30*(6), 414-421. Lingaswamy, K., Mohan, D., Krishna, P. R., & Prapurna, Y. L. (2016). Indium (III) Chloride Promoted Highly Efficient Tandem Rearrangement–α-Addition Strategy towards the Synthesis of α-Hydroxyamides. *Synlett*, *27*(11), 1693-1698.
15. Eigler, S., Grimm, S., Hof, F., & Hirsch, A. (2013). *Journal of Materials Chemistry A*, *1*, 11559-11562.
16. YAN, J. L., CHEN, G. J., Jun, C. A. O., Wei, Y., XIE, B. H., & YANG, M. B. (2012). Functionalized graphene oxide with ethylenediamine and 1, 6-hexanediamine. *New Carbon Materials*, *27*(5), 370-376. Ferreira, F. V., Brito, F. S., Franceschi, W., Simonetti, E. A. N., Cividanes, L. S., Chipara, M., & Lozano, K. (2018). Functionalized graphene oxide as reinforcement in epoxy based nanocomposites. *Surfaces and Interfaces*, *10*, 100-109. Shaabani, A., Sepahvand, H., Bazgir, A., & Khavasi, H. R. (2018). Tosylmethylisocyanide (TosMIC)[3+ 2] cycloaddition reactions: A facile Van Leusen protocol for the synthesis of the new class of spirooxazolines, spiropyrrolines and chromeno [3, 4-c] pyrrols. *Tetrahedron*, *74*(49), 7058-7067.
17. Krishnamoorthy, K., Veerapandian, M., Yun, K., & Kim, S. J. (2013). The chemical and structural analysis of graphene oxide with different degrees of oxidation. *Carbon*, *53*, 38-49.
18. Yang, D., Velamakanni, A., Bozoklu, G., Park, S., Stoller, M., Piner, R. D., ... & Ruoff, R. S. (2009). Chemical analysis of graphene oxide films after heat and chemical treatments by X-ray photoelectron and Micro-Raman spectroscopy. *Carbon*, *47*(1), 145-152. Díez-Betriu, X., Álvarez-García, S., Botas, C., Álvarez, P., Sánchez-Marcos, J., Prieto, C., ... & De Andrés, A. (2013). Raman spectroscopy for the study of reduction mechanisms and optimization of conductivity in graphene oxide thin films. *Journal of Materials Chemistry C*, *1*(41), 6905-6912.